Available online at www.sciencedirect.com
ScienceDirect
Journal of the European Ceramic Society 30 (2010) 243–247
www.elsevier.com/locate/jeurceramsoc

Photoluminescence and structural characteristics of double tungstates $A(M_{1-X}Pr_X)W_2O_8$ (A = Li, Cs, M = Al, Sc, La)

Kyoung Ho Lee [a], Ki-Woong Chae [b], Chae Il Cheon [a], Jeong Seog Kim [a,*]

[a] Dept. of BK21 Semiconductor & Display Engineering, Hoseo University, Baebang, Asan, Chungnam, 336-795, Republic of Korea
[b] Dept. of Materials Science and Engineering, Hoseo University, Baebang, Asan, Chungnam, 336-795, Republic of Korea

Available online 8 July 2009

Abstract

In this article, photoluminescence of Pr^{3+} ions in the double tungstate $A(M_{1-X}Pr_X)W_2O_8$ (A = Li, Cs, M = Al, Sc, La; $0.0 \leq X \leq 0.1$) are characterised. By varying ion radius in A and M sites the crystal structure was modified and even in crystals with similar structural characteristics three distinctive types of luminescence are observed. When the substitution ions in both A and M sites are relatively small the host lattice exhibits luminescence dominantly. With the small A site ion (Li^+) and the large M site ion (La^{3+}, 1.03 Å) the Pr^{3+} ion exhibits prominent luminescence. With the very large A site ion (Cs^+, 1.67 Å) and relatively small M site ion (Sc^{3+}, 0.75 Å) the Pr^{3+} exhibits both the $4f^2$–4f5d excitation and the ^3P_J manifold excitations in the absorption spectrum. These excitation levels lead to two strong emissions from the Pr^{3+}. PL characteristics are discussed with respect to crystal structural criteria.

Keywords: Powders solid state reaction (A); X-ray methods (B); Spectroscopy (B); Optical properties (C); Lamp envelopes (E)

1. Introduction

Photoluminescence of Pr^{3+} doped materials has many unique features such as quantum cutting (photon cascade emission), UV tuneable luminescence from $4f^15d^1$ levels, visible light emissions from $^3P_0$ and/or $^1D_2$ levels.[1,2] Quantum cutting phosphor producing two-photon emission by Pr^{3+} has been investigated as a promising candidate for an Hg-free Xe-discharge lamp and plasma display panels with high energy efficiencies.[3–5]

The Pr^{3+} ions in most oxides and fluorides emit blue-green and/or red light from $^3P_0$ level; blue-green lines at ~500 nm ($^3P_0 \rightarrow {}^3H_4$) and ~545 nm ($^3P_0 \rightarrow {}^3H_5$), and/or red lines at ~618 nm ($^3P_0 \rightarrow {}^3H_6$) and ~650 nm ($^3P_0 \rightarrow {}^3F_2$).[2–6] Contrarily, in some oxides the Pr^{3+} emits prominent red luminescence from $^1D_2$ level instead of the blue-green $^3P_0$ emissions: ~608 nm ($^1D_2 \rightarrow {}^3H_4$) and ~630 nm ($^1D_2 \rightarrow {}^3H_6$) lines.[1,7]

The wavelength and efficiency of red emissions from the Pr^{3+} ion are an important optical parameter in practical applications such as LED, PDP and discharge lamps. Radiationless de-excitation of the Pr^{3+} ion from the $^3P_0$ to the $^1D_2$ level, so-called '$^3P_0$ quenching', leads to the replacement of the $^3P_0$ blue-green emissions by $^1D_2$ red luminescence in some sesquioxides (Y_2O_3, La_2O_3) and transition metal oxides.[1,7] Multiphonon relaxation, $4f \rightarrow 4f$ cross-relaxation within pairs of Pr^{3+} ions and charge transfer states $4f^2 \rightarrow 4f^1L^1$ (L = ligand) via O^{2-} can provide the $^3P_0$ quenching pathways.[2–8] Since these processes are related to the structural characteristics of the host lattice, Okumura et al.[9] have suggested that the $^3P_0$ quenching criterion in terms of Pr^{3+}–O^{2-} bond distance is <2.4 Å in sesquioxides.

Boutinaud et al.[7] ascribed the $^3P_0$ quenching to a charge transfer state (CTS) [Pr^{4+}–O^{2-}–$M^{(n-1)+}$] closely low-lying in excitation energy state to the $4f^2$ [Pr^{3+}–O^{2-}–$M^{(n)+}$ configuration] (the $^3P_0$ level). The CTS mediates the $^3P_0$ quenching ($^3P_0$–$^1D_2$ radiationless de-excitation) in V- and Ti-oxides.[7,8] When electrons are transferred in a CTS, the electrons return to the $^1D_2$ excitation level of the Pr^{3+}. Relaxation of the $^1D_2$ level to ground state ($^1D_2$–$^3H_4$) emits red luminescence (~608 nm). Structural characteristics such as the Pr^{3+}–O^{2-}–M bond distance and orbital overlapping determine the relation of the CTS to the $^3P_0$ energy levels. Detailed coordinate diagrams regarding the relative positions of CTS, $^3P_0$ and 4f5d levels are given and discussed by Pinel et al.[1,7]

A modified structural criterion has been suggested by Pinel et al. based on the calculated point charge electrostatic potential value V as in Eq. (1) for some Pr^{3+} doped oxide materials.[1] They observed a complete $^3P_0$ quenching in the oxides showing

* Corresponding author. Tel.: +82 41 5405921; fax: +82 41 5405345.
E-mail address: kimjungs@hoseo.edu (J.S. Kim).

0955-2219/$ – see front matter © 2009 Elsevier Ltd. All rights reserved.
doi:10.1016/j.jeurceramsoc.2009.05.048

the calculated V to be smaller than +3.0 ($V<+3.0$). Moreover, the oxides with the calculated $V>+3.0$ showed a partial $^3P_0$ quenching.

$$V = -\sum_{i=1}^{N-} \frac{Z(-)}{R_i} + \sum_{j=1}^{N+} \frac{Z(+)}{R_j} \quad (1)$$

Here N− and N+ indicate the first and second nearest neighbours with charges Z− and Z+, respectively. R_i and R_j indicate bond distances to the first and second nearest neighbours.

In this equation, a high negative value of the first term is ascribed to either a short Pr^{3+}–O^{2-} distance or a large coordination number of O^{2-}. A high positive value of the second term implies a high coordination number of highly charged metal cations at a short distance.[1] Calculated V values for the Pr^{3+} ion in $SrMoO_4$ and $CaWO_4$ were ~+9.5.[1] These oxides exhibited the $^3P_0 + {}^1D_2$ lines indicating partial $^3P_0$ quenching.

The alkali double tungstate $ALnW_2O_8$ (A = Li, Na, K, Li, Ln = rare earth) has many advantageous optical properties useful in laser host materials and the phosphors of LED and X-ray detectors. However, the luminescence properties of the Pr^{3+} ion in this double tungstate have not been well understood.[11,12]

The alkali double tungstate $ALnW_2O_8$ has scheelite related structures with various crystal symmetries and lattice parameters.[10,11] In this study the crystal structure of the double tungstate $A(M_{1-X}\ Pr_X)W_2O_8$ (A = Li, Cs, M = Al, Sc, La) was modulated by substituting A and M sites with various ionic sizes (Å), e.g. $A = Li^+$ (0.53), Cs^+ (1.67), $M = Al^{3+}$ (0.53), Sc^{3+} (0.75), Y^{3+} (0.90) and La^{3+} (1.03). We report three distinct features of photoluminescence in these double tungstates. The characteristic luminescence behaviour of $A(M_{1-X}\ Pr_X)W_2O_8$ (A = Li, M = Al, Sc) is discussed with regard to the substitution ion size (Å) and the structural criterion based on the point charge potential V.

2. Experimental

The chemical composition of the tungstate samples was $A(M_{1-X}\ Pr_X)W_2O_8$ (A = Li, Cs, M = Al, Sc, La; $0.0 \le X \le 0.1$). All the samples were prepared by solid state reaction method. Chemically pure reagents, Li_2CO_3, La_2O_3, Pr_2O_3, Sc_2O_3, Al_2O_3, Cs_2CO_3 and WO_3 were used as the raw materials. Appropriate amounts of the raw materials were mixed thoroughly using a mortar with added ethyl alcohol and were then calcined in air at 600–700 °C for 5 h. The calcined powders were thoroughly reground and then fired at 800–1050 °C for 13 h in air. The fired samples were cooled in the furnace. The photoluminescence spectra of the fired samples were characterised using a vacuum ultraviolet PL measurement system (PS-PLUI-XWP1400, PSI). The X-ray diffraction data were obtained at room temperature using a DIMAX diffractometer. The point charge potential V for a known crystal structure was calculated using the software program WATOMS.

3. Results and discussion

In a scheelite structure such as AWO_4 (A = Ca, Ba), the host lattice complex (tetrahedral WO_4^{2-}) operates as the luminescence centre. Energy transition between O^{2-} 2p and W^{6+} 5d orbitals produces an electron–hole pair. The host lattice (WO_4^{2-}) emits blue-green light of a 440–540 nm wavelength range under an excitation source of 250–315 nm.[13,14] Scheelite related double tungstates of $LiRW_2O_8$ (R = Y, Pr) consist of both the tetrahedral (WO_4^{2-}) and octahedral (WO_6^{6-}) complexes.[13] Hence the host lattice as well as the Pr^{3+} ion can be the luminescence centres in $A(M_{1-X}\ Pr_X)W_2O_8$ (A = Li, Cs, M = Al, Sc, La).

The PL spectrum of the $Li(Al_{1-X}\ Pr_X)W_2O_8$ ($X = 0.0$–0.03) is shown in Fig. 1. A broad absorption band is observed centred at 281 nm, over which range both the WO_4^{2-} host lattice and $4f^2$–4f5d excitation peaks are usually observed.[3,4,15] Since the luminescence intensities of the absorption and emission bands are independent of Pr^{3+} doping contents, the $Li(Al_{1-X}\ Pr_X)W_2O_8$ can be taken to be the host lattice (WO_4^{2-}) luminescence. In the emission spectrum the Pr^{3+} $^3P_0$ lines are shown for comparison with the host lattice emission.

$Li(Sc_{1-X}\ Pr_X)W_2O_8$ ($X = 0.0$–0.04) also shows host lattice luminescence similar to that of the $Li(Al_{1-X}\ Pr_X)W_2O_8$. As summarised in Table 1, it has a broad absorption and emission bands at 295 and 484 nm, respectively. In addition to the host lattice luminescence, some weak lines from the Pr^{3+} $^3P_0$ level are observed.

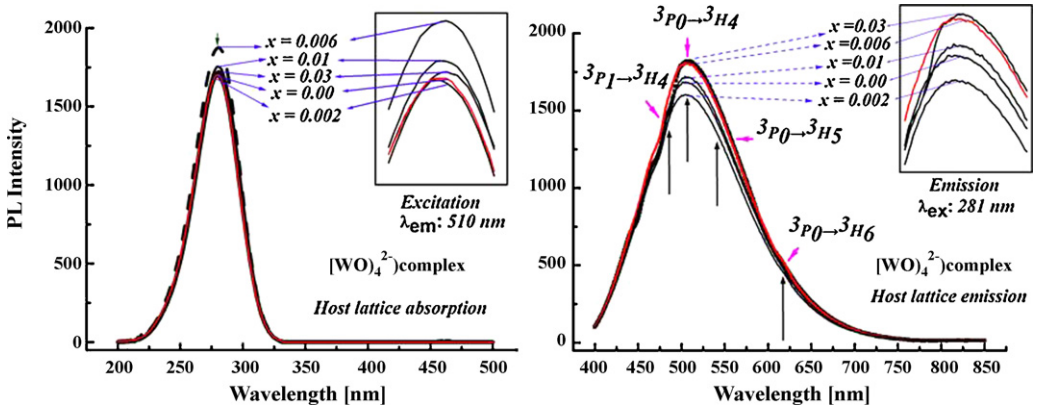

Fig. 1. PL spectrum of the $Li(Al_{1-X}\ Pr_X)W_2O_8$ ($X = 0.0$, 0.002, 0.006, 0.01, 0.03). The excitation spectrum was measured while observing the emission line at 510 nm. The emission spectrum was measured under the 281 nm excitation.

Table 1
Structure and photoluminescence property of $A(M_{1-X}\ Pr_X)W_2O_8$ (A = Li, Cs, M = Al, Sc, La, $0.0 \le X \le 0.1$).

Composition (ionic radius, Å)	Lattice parameters (Å), SG	Excitation peaks: relative intensity[a]	Emission peaks: relative intensity[a]
A = Li(0.53), M = Al(0.53)	JCPDS 28-0025 Monoclinic (unknown)	(1) Host excitation (281nm): s Only host lattice	(1) Host emission (510 nm): s Only host lattice
A = Li, M = Sc(0.75)	$a = 9.26$, $b = 11.38$, $c = 4.91$, $\beta = 90.3$, C2/c	(1) Host (295nm): s (2) Pr^{3+} 4f–4f transition: w ^3P_J ($J = 0, 1, 2$) manifold	(1) Host (484 nm): s (2) $^3P_0$ emission: w $^3P_0$–$^3H_6$, $^3P_0$–$^3H_4$ (495 nm)
A = Li, M = La(1.03)	$a = b = 5.28$, $c = 11.46$, $I4_1/a$	(1) 4f–4f transition: s ^3P_J ($J = 0, 1, 2$) (2) Host and $4f^2$–4f5d: vw	(1) $^3P_0$ emission $^3P_0$–$^3F_2$: s $^3P_0$–$^3H_4$: m $^3P_0$–$^3H_6$: w (2) $^1D_2$–$^3H_4$ emission: w
A = Cs(1.67), M = Sc	$a = 5.73$, $b = 7.90$, $c = 5.46$, $\beta = 115.4$, Monoclinic	(1) $4f^2$–4f5d (263nm): s (2) $^1S_0$–$^1I_6$: s (3) ^3P_J manifold: s (4) Host (281nm): w	(1) $^3P_0$–$^3H_6$: s (2) $^1D_2$–$^3H_4$: s (3) Host: w

[a] Relative intensity of luminescence lines; strong (s), medium (m), weak (w), very weak (vw).

Differently from the previous samples, $Li(La_{1-X}\ Pr_X)W_2O_8$ ($X = 0.007$–0.1) shows narrow excitation lines of Pr^{3+} 4f–4f transitions (^3P_J manifold) at 450–480 nm.[3,4,6] Both the host lattice and the $4f^2$–4f5d excitations are very weak as shown in Fig. 2. The $^3P_0$ level emits the strongest red line at 650 nm ($^3P_0$–$^3F_2$). In addition, a weak red line from the $^1D_2$ at 605 nm ($^1D_2$–$^3H_4$) was observed.

The $Cs(Sc_{1-X}\ Pr_X)W_2O_8$ ($X = 0.0 \sim 0.04$) exhibits substantially different luminescence behaviour than does the $Li(La_{1-X}\ Pr_X)W_2O_8$. The Pr^{3+} $4f^2$–4f5d excitation[14] in addition to ^3P_J manifold excitations are characteristically observable in the absorption spectrum as shown in Fig. 3. The narrow line at ~395 nm is presumed to be from Pr^{3+} $^1S_0$–$^1I_6$ [3–5], because the un-doped sample ($X = 0.0$) does not show this line. Energy transitions between the 4f5d–$^1S_0$ level and the intra-configurational 4f–4f transition ($^1S_0$–$^1I_6$) of Pr^{3+} has been reported by Kück et al.[3–5] in detail. The emission spectrum of the $Cs(Sc_{1-X}\ Pr_X)W_2O_8$ ($X = 0.007$–0.04) consists of two strong red emissions at 616 nm ($^3P_0$–$^3H_6$) and 605 nm ($^1D_2$–$^3H_4$). The host lattice luminescence is very weak. The strong intensity of the 605 nm line ($^1D_2$–$^3H_4$) indicates that the $^3P_0$ quenching to $^1D_2$ level occurred substantially in this sample.

Crystal phase analysis by XRD for the $A(M_{1-X}\ Pr_X)W_2O_8$ (A = Li, Cs, M = Al, Sc, La) samples is shown in Figs. 4 and 5. Fig. 4 shows the XRD patterns of $Li(Al_{0.99}Pr_{0.01})W_2O_8$ and $Li(La_{0.95}Pr_{0.05})W_2O_8$. The diffraction peaks of $Li(Al_{0.99}Pr_{0.01})W_2O_8$ can be indexed by JCPDS 28-0025 (β-$LiAlW_2O_8$). The structural detail of this double tungstate is not known yet, but can be presumed to be monoclinic, a crystal system to which many double tungstates belong. The diffraction peaks of $Li(La_{0.96}Pr_{0.04})W_2O_8$ are indexed by JCPDS 85-0443 of the tetragonal structure $CaWO_4$ ($I4_1/a$) as shown in upper part of Fig. 4.

Fig. 5 shows the XRD patterns of the $Li(Sc_{1-X}\ Pr_X)W_2O_8$ ($X = 0.0, 0.04$) and $Cs(Sc_{1-X}\ Pr_X)W_2O_8$ ($X = 0.0, 0.04$). In upper part the diffraction peaks of the $Li(Sc_{1-X}\ Pr_X)W_2O_8$ are indexed by JCDPS 72-0751 ($LiFeW_2O_8$, SG C2/c). The analysed lattice parameters are summarised in Table 1. In the lower part the $Cs(Sc_{1-X}\ Pr_X)W_2O_8$ patterns are indexed by a monoclinic cell ($a = 5.728$Å, $b = 7.896$Å, $c = 5.458$Å, $\beta = 115.4°$) calculated using the TREOR software program.

Presently crystal structural information on the double tungstate in this study is insufficient for clearly testing the structural criterion for the $^3P_0$. But it is worthwhile to discuss the PL

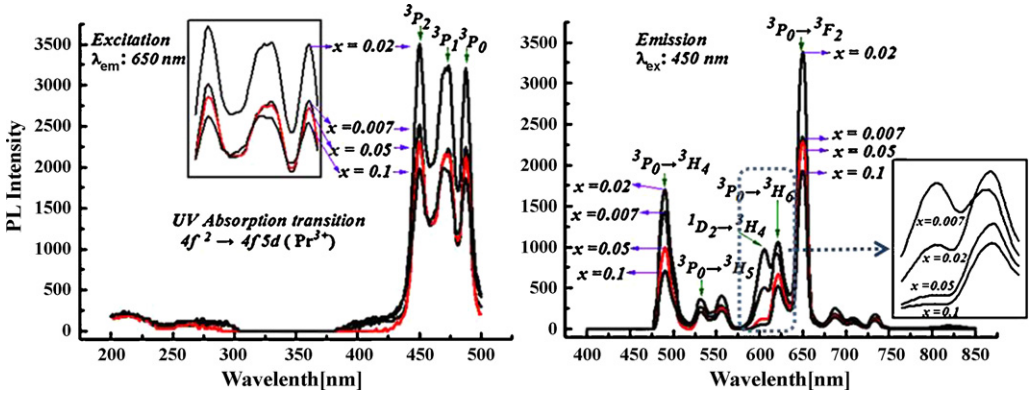

Fig. 2. PL spectrum of the $Li(La_{1-X}\ Pr_X)W_2O_8$ ($X = 0.007$, 0.02, 0.05, 0.1). The excitation spectrum was measured while observing the emission at 650 nm. The emission spectrum was measured at the 450 nm excitation.

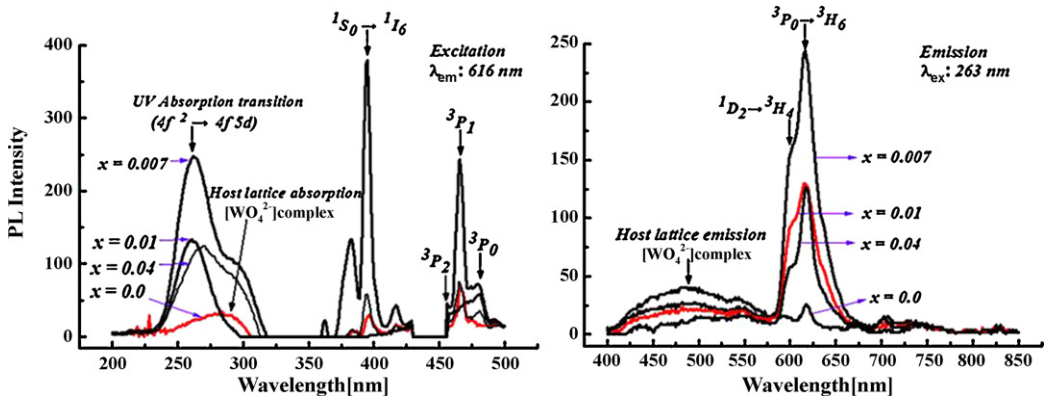

Fig. 3. PL of the $Cs(Sc_{1-X}\ Pr_X)W_2O_8$ ($X = 0.0$, 0.007, 0.01, 0.04). The excitation spectrum was measured while observing the 650 nm emission. The emission spectrum was measured under the 450 nm excitation.

characteristics with regard to the ion size (Å) in A and M sites, and the point charge potential V of the Pr^{3+}.

Three distinctive types of PL behaviours observed in $A(M_{1-X}\ Pr_X)W_2O_8$ (A = Li, M = Al, Sc) are summarised in Table 1. When the A site ion is small ($A = Li^+$, 0.53) and the M site ion is also small (or medium sized) [$A = Li^+(0.53)$, $M = Al^{3+}(0.53)/Sc^{3+}(0.75)$], the samples [$A(M_{1-X}\ Pr_X)W_2O_8$ (A = Li, M = Al, Sc)] become a host lattice for luminescence. With the small A site ion ($A = Li^+$, 0.53) and large M site ion ($M = La^{3+}$, 1.03), the sample [$Li(La_{1-X}\ Pr_X)W_2O_8$] exhibits Pr^{3+} 4f–4f excitation (^3P_J manifold) and $^3P_0$ emissions with scarce $^3P_0$ quenching. In the other sample $Cs(Sc_{1-X}\ Pr_X)W_2O_8$ with the very large A site ion ($A = Cs^+$, 1.67) and the moderate M site ion ($M = Sc^{3+}$, 0.745), both the Pr^{3+} $4f^2$–4f5d and ^3P_J manifold excitations occur. These excitation levels lead to two strong emissions of $^3P_0$–$^3H_6$ (616 nm) and $^1D_2$–$^3H_4$ (605 nm).

The point charge potential V of Pr^{3+} ions in the $Li(La_{1-X}\ Pr_X)W_2O_8$ ($X = 0.007$–0.1) would be ∼+9.0, since this sample has the same space group and similar lattice parameters as $CaWO_4$.[1] The V value of $Li(Sc_{1-X}\ Pr_X)W_2O_8$ is calculated as ∼+12 using the structural parameters of $LiFeW_2O_8$. The other sample, $Cs(Sc_{1-X}\ Pr_X)W_2O_8$, is supposed to also have a large positive V value due to the highly charged W^{6+} ion and large co-ordinations (6 or 8 CN) around the M site in the structure.[14] Hence the point charge potential V of the Pr^{3+} ion in the $A(M_{1-X}\ Pr_X)W_2O_8$ (A = Li, M = Al, Sc) can be presumed to have the same order of ∼+10.

Even when the order of the V values is similar, the double tungstates in this study show substantially different PL characteristics. The host lattice luminescence of the $A(M_{1-X}\ Pr_X)W_2O_8$ (A = Li, M = Al, Sc) samples ($V \sim +10$) has little relation with regard to the criterion. The $Li(La_{1-X}\ Pr_X)W_2O_8$ ($X = 0.007$–0.1) with $V = \sim +9.0$ conforms to the structural criterion[1] for the partial $^3P_0$ quenching and hence the luminescence shows both the $^3P_0$ (strong $^3P_0$–$^3F_2$ line) and the $^1D_2$ (weak $^1D_2$–$^3H_4$ line).

For the $Cs(Sc_{1-X}\ Pr_X)W_2O_8$ sample we would suggest that the characteristic $4f^2$–4f5d excitation and population of $^1S_0$ level led to $^1D_2$–$^3H_4$ (605 nm) emission independently of the $^3P_0$ quenching. In this route a de-excitation to $^1D_2$ level can be attained by 4f5d–$^1S_0$–$^1D_2$ and/or $^1S_0$–$^1D_2$ (∼400 nm) transition.

Further analytical work needs to be carried out on the detailed structural environment around the Pr^{3+} ion, W–O complex type

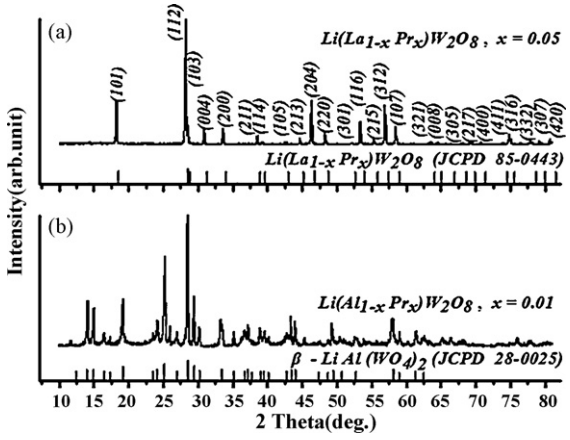

Fig. 4. XRD patterns of the $Li(M_{1-X}\ Pr_X)W_2O_8$ (M = Al, La). The upper pattern (a) is indexed by JCPDS 85-0443 ($CaWO_4$, $I4_1/a$). The lower pattern (b) is indexed by JCPDS 28-0025 (β-$LiAlW_2O_8$).

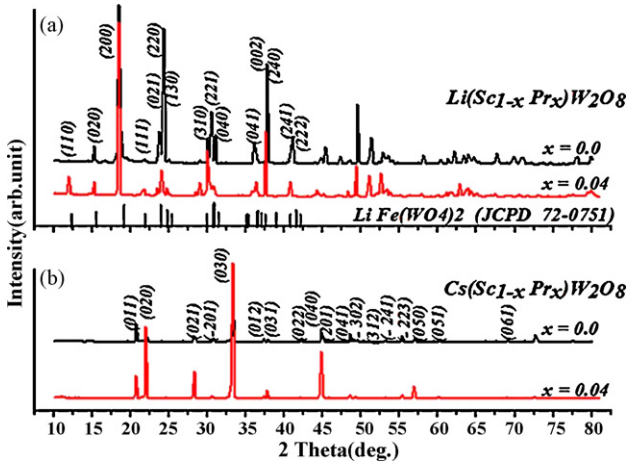

Fig. 5. XRD patterns of the $A(Cs_{1-X}\ Pr_X)W_2O_8$ (A = Li, Cs). Two patterns in the upper part (a) are indexed by JCDPS 72-0751 ($LiFeW_2O_8$, C2/c). The lower two patterns (b) are indexed by a monoclinic unit cell ($a = 5.728$Å, $b = 7.896$Å, $c = 5.458$Å, $\beta = 115.4^\circ$) calculated by TREOR program.

and the relation between the host lattice and Pr^{3+} excitations which divide the double tungstate into three distinct PL characteristic types.

4. Conclusion

The double tungstate $A(M_{1-X}\ Pr_X)W_2O_8$ (A = Li, M = Al, Sc) has a similar order of point charge potential values ($V \sim +10$) due to a highly charged W^{6+} ion and large co-ordinations (6 or 8 CN) around the M site. Even for similar V values three distinctive features of luminescence were observed by us among the double tungstates. When the A site ion is small ($A = Li^+$, 0.53) and the M site ion is small (or moderate) in size [$M = Al^{3+}(0.53)/Sc^{3+}(0.75)$], the double tungstate becomes a host for lattice luminescence consisting of broad absorption and emission bands. With a small A site ion ($A = Li^+$, 0.53) and a large M site ion ($M = La^{3+}$, 1.03), the tungstate exhibits Pr^{3+} 4f–4f excitation (^3P_J manifold) and $^3P_0$ emissions with scarce $^3P_0$ quenching. When the A site ion is very large ($A = Cs^+$, 1.67) and the M site ion is moderately sized ($M = Sc^{3+}$, 0.75), the double tungstate shows coexistence of the Pr^{3+} $4f^2$–4f5d and ^3P_J manifold excitations. These excitation levels lead to two strong emissions of the $^3P_0$–$^3H_6$ and $^1D_2$–$^3H_4$. Population of the excitation energy states, such as $4f^2$–4f5d excitation and $^1S_0$ level can be a possible route leading to $^1D_2$–$^3H_4$ emission independently of $^3P_0$ quenching in $Cs(Sc_{1-X}\ Pr_X)W_2O_8$. Further study on the crystal structural environment around the Pr^{3+} ion, and on the relative coordinates between host lattice excitation and optical energy levels of Pr^{3+}in the double tungstate are necessary.

Acknowledgement

This work was supported by grant no. RTI04-01-02 from the Regional Technology Innovation Program of the Ministry of Commerce, Industry and Energy (MOCIE).

References

1. Pinel, E., Boutinaud, P. and Mahiou, R., Using a structure criterion for selection of red-emitting oxide-based compounds containing Pr^{3+}. *J. Alloys Compd.*, 2004, **374**, 165–168.
2. Wegh, R. T., Donker, H., Oskam, K. D. and Meijerink, A., Visible quantum cutting in $LiGdF_4:Eu^{3+}$ through downconversion. *Science*, 1999, **283**, 663–666.
3. Vink, A. P., Dorenbos, P. and van Eijk, C. W. E., Observation of the photon cascade emission process under $4f^15d^1$ and host excitation in several Pr^{3+}-doped materials. *J. Solid State Chem.*, 2003, **171**, 308–312.
4. Kück, S., Sokólska, I., Henke, M., Döring, M. and Scheffler, T., Photon cascade emission in Pr^{3+}-doped fluorides. *J. Lumin.*, 2003, **102–103**, 176–181.
5. Srivastava, A. M., Doughty, D. A. and Beers, W. W., On the vacuum-ultraviolet excited luminescence of Pr^{3+} in LaB_3O_6. *J. Electrochem. Soc.*, 1997, **144**, L190–L192.
6. Gong, X., Xiong, F., Lin, Y., Tan, Q., Luo, Z. and Huang, Y., Crystal growth and spectral properties of $Pr^{3+}:La_2(WO_4)_3$. *Mater. Res. Bull.*, 2007, **42**, 413–419.
7. Boutinaud, P., Pinel, E., Oubaha, M., Mahiou, R., Cavalli, E. and Bettinelli, M., Making red emitting phosphors With Pr^{3+}. *Opt. Mater.*, 2006, **28**, 9–13.
8. Donega, C., De, M., Meijerink, A. and Blasse, G., Non-radiative relaxation process of the Pr^{3+} ion in solids. *J. Phys. Chem. Solids*, 1995, **56**, 673–675.
9. Okumura, M., Tamatani, M., Albessard, A. K. and Matsuda, N., Luminescence properties of rare earth ion-doped monoclinic yttrium sesquioxide. *Jpn. J. Appl. Phys.*, 1997, **36**, 6411–6415.
10. Yamamoto, H., Seki, S. and Ishiba, T., The Eu site symmetry in $AEu(MoO_4)_2$ (A = Cs or Rb) generating saturated red luminescence. *J. Solid State Chem.*, 1991, **94**, 396–403.
11. Van Vliet, J. P. M., Blasse, G. and Brixner, L. H., Luminescence properties of alkali europium double tungstates and molybdates $AEuM_2O_8$. *J. Solid State Chem.*, 1988, **76**, 160–166.
12. Macalik, L., Hanuza, J., Sokolnicki, J. and Legendziewicz, J., Optical properties of Pr^{3+} in lanthanum double molybdates and tungstates: $KLa_{1-X}Pr_X(MO_4)_2$ (M = Mo,W; $X \leq 1$). *Spectrochim. Acta*, 1999, **55**, 251–262.
13. Lou, Z. and Cocivera, M., Cathodluminescence of $CaWO_4$ and $SrWO_4$ thin films prepared by spray pyrolysis. *Mater. Res. Bull.*, 2002, **37**, 1573–1582.
14. Yen, W. M., Shionoya, S. and Yamamoto, H., Principal phosphor materials and their optical properties. *Phosphor Handbook*. CRC Press, New York, 1998, pp. 293–338, Chapter 3.
15. Kim, J. S., Lee, J. C., Cheon, C. I. and Kang, H.-J., Crystal structures and low temperature cofiring ceramic property of $(1-x)(Li,RE)W_2O_8$–$xBaWO_4$ ceramic (RE = Y,Yb). *Jpn. J. Appl. Phys.*, 2006, **45**, 7397–7400.